PHYSICAL REVIEW B **76**, 161403(R) (2007)

Experimental evidence for two-dimensional magnetic order in proton bombarded graphite

J. Barzola-Quiquia,[1] P. Esquinazi,[1,*] M. Rothermel,[1] D. Spemann,[1] T. Butz,[1] and N. García[2]
[1]*Institut für Experimentelle Physik II, Universität Leipzig, Linnéstraße 5, D-04103 Leipzig, Germany*
[2]*Laboratorio de Física de Sistemas Pequeños y Nanotecnología, Consejo Superior de Investigaciones Científicas, E-28006 Madrid, Spain*

(Received 29 June 2007; published 16 October 2007)

We have bombarded graphite samples with protons at low temperatures and low fluences to attenuate the large thermal annealing produced during irradiation. The overall optimization of sample handling allowed us to find Curie temperatures $T_c \gtrsim 350$ K at the fluences used. The magnetization versus temperature shows unequivocally a linear dependence, which can be interpreted as due to excitations of spin waves in a two-dimensional Heisenberg model with a weak uniaxial anisotropy.

DOI: 10.1103/PhysRevB.76.161403 PACS number(s): 75.50.Pp, 75.30.Ds, 78.70.−g

Recent advances in developing nanographitic systems have led to a worldwide renewed interest in their electrical properties.[1] A single layer of graphite, the two-dimensional (2D) graphene, appears to have quantum properties at room temperature[2] as well as rectifying electronic properties.[3,4] On the other hand those properties have already been observed in highly oriented pyrolytic graphite (HOPG) of low mosaicity, as the quantum Hall effect,[5] and de Haas–van Halphen quantum oscillations even at room temperature.[6] The two-dimensional properties of the graphene planes in graphite open up the possibility of using nanometer to micrometer sized regions of graphite in new integrated devices with spintronic properties, through the use of ferromagnetic electrodes, e.g., spin valves, and/or by making graphite itself magnetic. In fact this has been a topic of study in recent years, and reports exist showing magnetic hysteresis in clean graphite[7] but especially in proton bombarded graphite.[8] Severe limitations in the sensitivity and reproducibility of standard magnetometers, added to annealing effects during bombardment, hindered the identification of the critical temperature T_c as well as the characteristics and dimensionality of the ferromagnetic signals. The aim of this work is to show that specially prepared highly oriented pyrolytic graphite samples show ferromagnetic order with $T_c \gtrsim 350$ K, and the magnetization temperature dependence is in good agreement with a 2D anisotropic Heisenberg model (2DHM) and the presence of spin-wave excitations.[9–11]

For the experiments we used four pieces of a HOPG sample grade ZYA (rocking curve width 0.4°), samples 1–4 (mass 12.8, 12.5, 10.1, and 6 mg, respectively) irradiated by a 2.25 MeV proton microbeam (sample 4, 2.0 MeV, 0.8-mm-broad beam) perpendicular to the graphite planes. With the microbeam we produced several thousands of spots of ~ 2 μm diameter each and separated by a distance 5 μm (sample 1) or 10 μm (samples 2 and 3), similarly to the procedure used in Ref. 12. Samples 1 and 2 were irradiated at 110 K and samples 3 and 4 at room temperature. Further irradiation parameters for sample 1 (2, 3, 4) were 51 375 (25 600, 25 600, 6) spots, fluence 0.124 (0.08, 0.13, 0.3) nC/μm^2, total irradiated charge 46.9 (44.8, 37.4, 900) μC, and 1 nA proton current (100 nA for sample 4). The pieces we have irradiated showed an iron concentration (the only detected magnetic impurity) within the first 35 μm of $\sim 0.4 \pm 0.04$ μg/g (<0.1 ppm).

Previous experiments[8] showed ferromagnetic magnetic moments at saturation $m_{sat} \sim 1$ μemu and therefore put severe constraints on experimentalists, regarding not only the sensitivity of the magnetometer used but also its reproducibility after sample handling. In this work two main experimental improvements have been achieved. First, we enhanced the ferromagnetic part produced by irradiation, reducing annealing effects. In samples 1 and 2 the micrometer spots were produced at a nominal temperature of 110 K during irradiation (18 h). For comparison and to reduce further annealing effects, sample 4 was irradiated with a broad beam and low fluence. Second, we have designed a sample holder that allows us to measure the magnetic moment of the sample in the superconducting quantum interference device (SQUID) and to fix it inside the irradiation chamber without any changes. We investigated the reproducibility of the magnetic measurements and checked that the sample holder handling (with sample),[13] i.e., inserting it into and taking it out of the irradiation and SQUID chambers,[14] does not produce systematic changes of the magnetic signal. Our arrangement provides a reproducibility of $\sim 10^{-7}$ emu in the measured field range and allows the subtraction of the virgin data from those after irradiation point by point, substantially increasing the sensitivity of the magnetic measurements to $\sim 2 \times 10^{-8}$ emu.

Figure 1 shows the hysteresis loops of the magnetic moment m of sample 2 at two temperatures. These loops are obtained directly from the difference of the measurements after and before irradiation. The loop at 5 K as well as the measured temperature dependence at constant field indicate a paramagnetic contribution $m_p = 0.575 H/T$ μemu K/kOe for this sample, i.e., less than 10% of the ferromagnetic signal at 3 kOe. At 300 K, however, m_p is negligible. These loops and their temperature dependence, as well as the finite hysteresis (see the inset in Fig. 1), indicate the existence of magnetic order with a Curie temperature higher than room temperature.

Sample 3, which was irradiated with a similar number of spots, fluence, and total charge but at room temperature, shows a a ferromagnetic signal at saturation $\sim$ five times smaller than that obtained for samples 1 or 2, in agreement with previous work.[8] These results indicate the reliability and

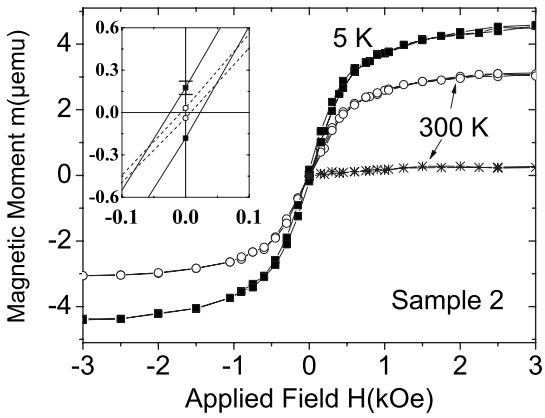

FIG. 1. Magnetic moment as a function of applied field for the irradiated sample 2 at 300 (○) and 5 K (■) obtained after subtracting the data for the nonirradiated sample. The points (⋆) are obtained for the same sample at 300 K after taking out the first ~5 μm from the irradiated surface side. The inset blows up the data at low fields to show the finite hysteresis and the clear temperature dependence of the coercive field and remanent magnetic moment.

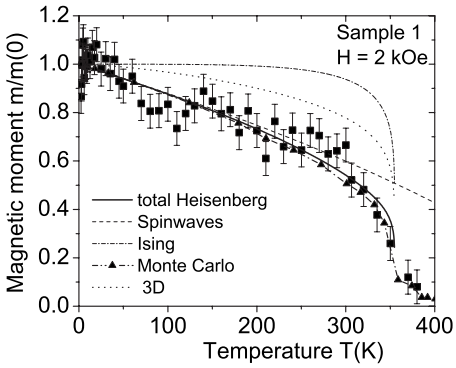

FIG. 2. Normalized magnetic moment $[m(0)=2.60\ \mu\text{emu}]$ obtained for irradiated sample 1 at 2 kOe. The data points are obtained after subtracting the data from the sample before irradiation and a paramagnetic (Curie) contribution $m_p(T)=4.9/T\ \mu$emu K. The errors bars indicate typical errors due to the subtraction of the data from the virgin sample. The chosen parameters for the theoretical curves are $T_c=360$ K, $T_c^{sw}=850$ K ($\Delta=0.001$). The continuous line is obtained from (1). The dotted line is the 3D Bloch $T^{3/2}$ model with spin waves (Ref. 18). The dash-dotted line with close triangles shows the results of a Monte Carlo simulation with anisotropy (square lattice of 200×200 points).

sensitivity of the used procedure as well as the absence of obvious artifacts in the measurements.

After removing the first few micrometers from the irradiated surface of sample 2, the ferromagnetic contribution decreased by one order of magnitude (see Fig. 1). We can now answer the question of whether the Fe concentration in the sample, due to some hypothetical annealing by the protons, could be responsible for the observed ferromagnetic signal. In the first micrometer depth and, following Ref. 15 and electrostatic force microscopy characterization of sample 2, taking an irradiated magnetic area of ring shape around the center of the spot of $\lesssim0.026$ cm^2, the magnetization at room temperature is then $\gtrsim5$ emu/g. In this region we estimate that the mass of the ferromagnetic carbon material is $<0.6\ \mu$g. Were the measured Fe concentration ferromagnetic at 300 K, then it would contribute with a magnetic moment $\lesssim0.6\times10^{-11}$ emu, i.e., 5×10^5 times smaller than the measured one. Given the mass of the ferromagnetic part of the irradiated HOPG sample, we estimate a magnetic moment per carbon atom of $m_C\sim0.01\mu_B$, in very good agreement with X-ray magnetic circular dichroism results.[15]

Figures 2 and 3 show the temperature dependence of the ferromagnetic moment for samples 1 and 4, respectively. Because the paramagnetic signal contributes significantly only at $T\lesssim25$ K, we have subtracted it in both figures in order to show only the ferromagnetic part. Up to the highest measured temperature of 380 K, this magnetic moment behaves reversibly. Furthermore, no changes in m within experimental error were observed after leaving the samples for several months at room temperature.

One of the interesting and indicative results shown in Figs. 2 and 3 is the unequivocal linear dependence. This is an indication of 2D magnetism, and the slope can be interpreted as due to the excitation of 2D spin waves that reduce the magnetization linearly with T.[9–11] We are not aware of any model Hamiltonian producing such a linear behavior in $m(T)$. Therefore, to analyze the measured temperature dependence we discuss the 2DHM with anisotropy that provides a linear dependence on T. The discrete Hamiltonian describing the 2DHM reads $H=-J\Sigma_{ij}[S_{iz}S_{jz}+(1-\Delta)(S_{ix}S_{jx}+S_{iy}S_{jy})]$, where $S_i=(S_{ix},S_{iy},S_{iz})$ represents a unit vector in the direction of the classical magnetic moment placed at the site i of a 2D lattice. The sum (i,j) is performed over all nearest-neighbor pairs, and J is the exchange coupling. The parameter Δ represents the uniaxial anisotropy in the z direction. The case $\Delta=0$ is the isotropic 2DHM and is known to have $T_c=0$. However, just a small anisotropy raises T_c considerably because $T_c\sim-1/\ln\Delta$ for $\Delta\to0$.

It can be shown [9–11] that the normalized spin-wave magnetization in the anisotropic axis behaves as $M_z^{sw}=1-T/T_c^{sw}-2T^2/(T^\star T_c^{sw})-(2/3)(T/T_c^{sw})^3$ at low tempera-

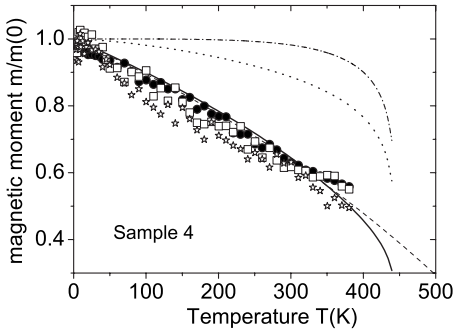

FIG. 3. Normalized magnetic moment $[m(0)=4.9\ \mu$emu at 10 kOe] obtained for sample 4 at (10,3,1) kOe (●, □, ⋆) after subtracting the data from the sample before irradiation and a paramagnetic (Curie) contribution $m_p(T)=1.18H/T\ \mu$emu K/kOe. The different theoretical curves are the same as in Fig. 2 but with parameters $T_c=450$ K and $T_c^{sw}=1050$ K.

tures, where $T^{\star}=4J$. This result is obtained using perturbation theory techniques[16,17] up to third order in spin waves. The parameter T_c^{sw} is the spin-wave critical temperature due to low-energy spin-wave excitations; it is given by $k_B T_c^{sw}=2\pi J/K(1-\Delta)$, where $K(x)$ is the elliptic function. Near the critical temperature T_c the physics can be better described by a 2D Ising model, which should provide a good description of the spin-flip excitations. Then T_c is given by $T_c(\hat{J})=1.52\hat{J}$,[16] where $\hat{J}$ is the renormalized exchange due to the spin-wave excitations according to the expression $\hat{J}(T)=J(1-2T/T_c^{sw})$. The values of M_z at $T<T_c$ can be expressed as

$$M_z(T) \approx M_z^{sw}(T,J)M_z^I[T,\hat{J}(T)]. \quad (1)$$

The first factor in the right-hand side of (1) is the magnetization due to spin waves, and the second one is the magnetization due to an Ising model with the exchange renormalized by the spin waves. We have checked this theoretical result against Monte Carlo calculations with $\Delta=0.001$ and the agreement is excellent, especially at low anisotropies,[11] as shown in Figs. 2 and 3. In Fig. 2 we have plotted also the normalized spin-wave (SW) contribution $M_z^{sw}/M_z^{sw}(0)$ up to third order. The Heisenberg result approximated by (1) and the Monte Carlo calculation agree, and both fit the experimental data with the parameters $T_c^{sw}=850$ K, $\hat{J}(T_c=360\ \mathrm{K})=237$ K, indicating an anisotropy $\Delta\simeq 0.001$. Sample 2 shows a similar behavior, and its data can be fitted with $T_c^{sw}\simeq 1000$ K, $\hat{J}(T_c\simeq 310\ \mathrm{K})=202$ K. The data for sample 4 shown in Fig. 3 also show a linear behavior. Extrapolating the SW contribution to $m(T^{\star})\simeq 0$, we conclude that $T_c<T^{\star}\simeq 640$ K. Then using (1) we estimate $T_c\gtrsim 450$ K with $\Delta\lesssim 10^{-4}$ (see Fig. 3). These results already show that T_c increases with fluence, provided that one can simultaneously reduce the annealing effects produced during irradiation. For comparison we have also plotted in Figs. 2 and 3 the Ising model result, which has no spin waves, and the 3D Bloch $T^{3/2}$ law that includes spin waves.[18] The comparison indicates clearly that spin waves in 2D dominate the magnetization up to $\gtrsim 300$ K and that the usual 3D model does not fit the data.

The previous analysis is for a periodic system of spins. Our irradiation process, however, generates disorder. Provided that this is not large enough to destroy the magnetic phase transition, as experimentally shown, then the following renormalization applies. With disorder the stiffness $2\langle S\rangle J$ changes to $2\langle S\rangle J(1-\{p/[1-(2/z)]\})$, where $0\leq p\leq p_c$; $p=0$ means no disorder; p_c is a critical percolation disorder parameter ($p_c\approx 0.4$) above which there is no spontaneous magnetization; and z represents the nearest-neighbor number.[19,20] The effective stiffness that fits the experiment should take this renormalization into account. We stress, however, that the temperature law of the magnetization remains linear for a 2D spin system with disorder, since this law is described by the spin-wave occupation number.

Defects in the graphite structure are one of the possible origins for localized magnetic moments. The ferromagnetism triggered by the bombardment should be correlated to the produced defects located in approximately the first micrometer from the sample surface. To discuss the mechanism responsible for the coupling between the magnetic moments, we need first to estimate the density of defects. For sample 1 we have 0.9 nC total irradiated charge per spot in an area of $\sim\pi 0.6^2\ \mu\mathrm{m}^2$. Using SRIM2003 Monte Carlo simulations with full damage cascades and 35 eV displacement energy, we obtain a vacancy density of $\sim 5\times 10^{20}\ \mathrm{cm}^{-3}$ at the surface, which means a distance between vacancies of $l\sim 1.3$ nm $\sim 9a$, where $a=0.14$ nm. This distance is much smaller than the inverse of the Fermi wave vector $1/k_F\sim 30$ nm for a Fermi energy of 20 meV or that calculated using the 2D carrier density.[5]

Regarding the coupling needed to have room-temperature magnetic ordering, there is in the first place direct coupling for nearly localized spins at the defects, which should be in the range of ~ 300 K. Recently, Ruderman-Kittel-Kasuya-Yosida (RKKY) coupling between large defects in graphene has been studied for Fermi energy tending to zero.[21] This coupling might be always ferromagnetic because $k_F r\ll 1$ for $r\sim l$. However, estimations of the Curie temperature for this coupling within our defect densities provide values of the order of 20 K. What appears important is a superexchange mediated by the two different sites in the graphite lattice[22,23] or between magnetic moments from defects and from hydrogen atoms, which may effectively increase the magnetic moment density on a graphene lattice.

We note that a large concentration of hydrogen is found in the region within 1 μm of the surface of graphite samples.[24] Therefore we should take into account the possible influence of hydrogen in triggering localized as well as nonlocalized magnetic moments in the graphite layers.[22,25] Irradiation may contribute to defect generation as well as in dissociating the existing molecular hydrogen, enabling its diffusion and bonding in defective parts of the lattice structure. All these moments will tend to be ferromagnetically coupled, enhancing the Curie temperature by the RKKY coupling.

Within this picture, it becomes clear that the enhancement of the defect density, which occurs at larger depths from the surface in the inner part of the irradiation path up to full amorphization at a depth $\sim 35-40\ \mu$m, perturbs the graphene lattice too much destroying in this way the necessary band structure and carrier density. This may explain the experimental observation of a rather well-defined critical temperature (and not a distribution) and also the difficulty one has in reaching much higher ferromagnetic magnetization values by increasing the proton fluences clearly above the values used here. If an electron-mediated coupling between defects plays a role, we expect that for an adequate defect density it should be possible to influence the magnetic order, shifting the Fermi energy by applying an appropriate bias voltage.

The results of samples 1 and 2 provide clear evidence for the good reproducibility of our approach: although the spot density, beam diameter, and total charges were different, the defect densities produced in the irradiated paths were similar for both samples, and therefore we expect to obtain similar critical temperatures, as the measurements showed. By changing the defect density as well as their distribution in the lattice, one may tune the ferromagnetic transition tempera-

ture as well as the magnitude of the magnetization produced by irradiation, as the data for sample 4 clearly indicate. As a rule of thumb, robust ferromagnetism with $T_c > 300$ K can be reached by proton irradiation in graphite with fluences of the order of 0.1 nC/μm^2.

In conclusion, our work shows that irradiation of micrometer spots in graphite at low temperatures as well as broad irradiation, both at very low fluences, increase significantly the magnitude of the magnetic order with Curie temperatures $T_c \gtrsim 300$ K. The use of special sample holders made it possible to reduce sample handling between irradiation chambers and SQUID measurements to a minimum, ruling out simple introduction of impurities or the influence of operative artifacts. This approach substantially increased the sensitivity and reproducibility of the magnetization measurements, allowing us to obtain directly the effects produced by irradiation within an error of $\sim 10^{-7}$ emu. The experimental localization of the ferromagnetic irradiated part of the sample indicates that the graphite structure is important, and that at the proton energies used low fluences are preferential to trigger a robust ferromagnetic order. We showed that the magnetization of the magnetically ordered contribution decreases linearly at $T < T_c$, a behavior that can be assigned to the signature of low-energy spin-wave excitations well described by a uniaxial two-dimensional anisotropic Heisenberg model.

We gratefully acknowledge discussions with M. A. Vozmediano and L. Pisani and K. Schindler for the microscopic characterization of the spots. This work was done in the framework of the EU project "Ferrocarbon" and partially supported by the DFG under Grant No. ES 86/11-3.

*esquin@physik.uni-leipzig.de

[1] See, for example, the review by M. I. Katsnelson, Mater. Today **10**, 20 (2007).
[2] K. S. Novoselov *et al.*, Science **315**, 1379 (2007).
[3] K. S. Novoselov *et al.*, Science **306**, 666 (2004).
[4] Y. Zhang, J. P. Small, M. E. S. Amori, and P. Kim, Phys. Rev. Lett. **94**, 176803 (2005).
[5] Y. Kopelevich, J. H. S. Torres, R. R. da Silva, F. Mrowka, H. Kempa, and P. Esquinazi, Phys. Rev. Lett. **90**, 156402 (2003). R. Ocaña, P. Esquinazi, H. Kempa, J. H. S. Torres, and Y. Kopelevich, Phys. Rev. B **68**, 165408 (2003); H. Kempa, P. Esquinazi, and Y. Kopelevich, Solid State Commun. **138**, 118 (2006).
[6] H. Kempa *et al.*, Solid State Commun. **115**, 539 (2000).
[7] P. Esquinazi, A. Setzer, R. Hohne, C. Semmelhack, Y. Kopelevich, D. Spemann, T. Butz, B. Kohlstrunk, and M. Lösche, Phys. Rev. B **66**, 024429 (2002).
[8] P. Esquinazi, D. Spemann, R. Hohne, A. Setzer, K. H. Han, and T. Butz, Phys. Rev. Lett. **91**, 227201 (2003). For a recent review see P. Esquinazi *et al.*, in *Carbon-Based Magnetism*, edited by T. Makarova and F. Palacio (Elsevier, Amsterdam, 2006), Chap. 19, p. 437.
[9] W. Doring, Z. Naturforsch. A **16**, 1008 (1961).
[10] A. P. Levanyuk and N. García, J. Phys.: Condens. Matter **4**, 10277 (1992).
[11] P. A. Serena, N. García, and A. P. Levanyuk, Phys. Rev. B **47**, 5027 (1993).
[12] K.-H. Han *et al.*, Adv. Mater. (Weinheim, Ger.) **15**, 1719 (2003).
[13] J. Barzola-Quiquia *et al.*, Nucl. Instrum. Methods Phys. Res. B **256**, 412 (2007).
[14] Our superconducting quantum interferometer device measurements were done using a reciprocal sample option, which increases the sensitivity by a factor of 10. The magnetic field was applied parallel to the graphene planes.
[15] H. Ohldag, T. Tyliszczak, R. Hohne, D. Spemann, P. Esquinazi, M. Ungureanu, and T. Butz, Phys. Rev. Lett. **98**, 187204 (2007).
[16] E. Brézin and J. Zinn-Justin, Phys. Rev. B **14**, 3110 (1976).
[17] D. R. Nelson and R. A. Pelcovits, Phys. Rev. B **16**, 2191 (1977).
[18] C. Kittel, *Introduction to Solid State Physics*, 7th ed. (John Wiley & Sons, New York, 1996), p. 455.
[19] S. Kirkpatrick, Rev. Mod. Phys. **45**, 574 (1972).
[20] R. C. Jones and G. J. Yates, J. Phys. C **8**, 1705 (1975).
[21] M. A. H. Vozmediano, M. P. López-Sancho, T. Stauber, and F. Guinea, Phys. Rev. B **72**, 155121 (2005).
[22] O. V. Yazyev and L. Helm, Phys. Rev. B **75**, 125408 (2007).
[23] L. Pisani, B. Montanari, and N. Harrison (unnpublished).
[24] P. Reichart *et al.*, Nucl. Instrum. Methods Phys. Res. B **249**, 286 (2006).
[25] P. O. Lehtinen, A. S. Foster, Y. Ma, A. V. Krasheninnikov, and R. M. Nieminen, Phys. Rev. Lett. **93**, 187202 (2004).